Version of Record: https://www.sciencedirect.com/science/article/pii/S0967064518300328
Manuscript_f4e430874b347eab6d334968b787ca18

Flow Patterns in the Chukchi Sea based on an Ocean Reanalysis, June through October 1979-2014

Nicholas Bond[a*], Phyllis Stabeno[b], Jeffrey Napp[c]

[a]University of Washington/JISAO, Seattle, WA 98105 USA
[b]NOAA Pacific Marine Environmental Laboratory, 7600 Sand Point Way NE, Seattle WA 98115-0070 USA
[c]NOAA Alaska Fisheries Science Center, 7600 Sand Point Way NE, Seattle WA 98115-0070 USA

*Corresponding author. Phone: (206) 526-6459; Fax: (206) 526-6485
Email: nab3met@u.washington.edu (N. Bond)

© 2018 published by Elsevier. This manuscript is made available under the Elsevier user license
https://www.elsevier.com/open-access/userlicense/1.0/

ABSTRACT

The oceanography of the Arctic is changing, with the potential to restructure the function and production of its ecosystems. The physical oceanographic conditions that have occurred on the Chukchi Sea shelf during June through October of the years 1979–2014 were investigated using the ORAS4 ocean reanalysis product. Time series of vertically integrated temperatures (especially during September and October) indicate greater warming in the first half of the 36-year record. This change in the long-term temperature trend may be in part due to trends in the mean currents, which in Herald Canyon and off the coast of Northwest Alaska tended to be slightly less poleward after 2000. A k-means cluster analysis of monthly mean sea-surface height anomaly distributions was used to describe five distinct patterns of flow. Two of the five patterns (clusters 2 and 4) relate to the strength of the Alaskan Coastal Current (ACC). Another pair of patterns (clusters 3 and 5) had their strongest expressions in the northwest Chukchi Sea and relate to periods of weak southeastward versus strong northwestward flow in this region associated with the presence or absence of the Siberian Coastal Current. The fifth pattern (cluster 1) was defined by weak southeastward flow anomalies in the western Chukchi and a slightly suppressed ACC relative to the mean in the eastern Chukchi Sea. The composite sea-surface height anomaly patterns of the five cluster types correspond closely with the mean sea level pressure anomaly distributions during the months constituting each cluster type. Our findings for the Chukchi Sea region provide a long-term context for previous field observations and may be useful for interpretation of past ecosystem variations.

Keywords: Chukchi Sea, temperature, long-term change, currents, sea surface height, ecosystem

1. Introduction

This paper provides a physical oceanographic perspective on the Chukchi Sea for this special issue, the second volume of the Synthesis Of Arctic Research (SOAR) program. Our objective is to describe the mean and variability in the regional scale flow during the months of June through October of 1979-2014, building upon previous studies for the area (e.g. Weingartner et al., 2005, 2013; Gong and Pickart, 2016). The mean flow through Bering Strait is northward, driven by difference in sea surface height (SSH) between the Pacific and Arctic Oceans (Aagaard et al., 2006). The average rate of transport through Bering Strait is approximately 1×10^6 m^3 s^{-1} (1 Sv) with considerable interannual variability (Woodgate et al., 2012; Woodgate et al., 2015). The general circulation on the Chukchi Sea shelf is also northward. The Chukchi flow divides principally into three branches associated with the bathymetry: Herald Canyon, Central Channel, and along the Alaskan coast (see Fig. 1 for the locations of these and other bathymetric features). Much of the Central Channel flow joins the coastal flow to exit the Chukchi Sea shelf through Barrow Canyon (e.g. Wang et al., 2014; Gong and Pickart, 2016). The total transport exiting via Barrow Canyon is ~0.4 Sv (5-year average, 2010–2015; Stabeno et al., 2017). The heat associated with this water source ultimately impacts sea-ice coverage in the Beaufort Sea (e.g. Shimada et al. 2006; Itoh et al. 2015). Along with the overall northward flow, at times a southeastward flow termed the Siberian Coastal Current (SCC) develops along the Siberian coast, eventually turning northward and joining the flow toward Herald Canyon (Weingartner et al., 1999). The SCC is ephemeral, with fluctuations on sub-seasonal to interannual time scales.

The currents throughout the Chukchi Sea vary on time scales ranging from days to years. The sub-seasonal variations in the currents through Bering Strait are primarily wind forced, with the strongest and weakest fluctuations typically in the months of winter and summer, respectively. The flow farther north on the Chukchi Sea shelf at Icy Cape is of a similar nature, with maximum flow in the summer and maximum variability in the winter months (Stabeno et al., 2016). Reversals of flow can occur throughout the year, with the strongest reversals typically in winter. Reversals from the usual northeastward flow in Barrow Canyon can result in the transport of Atlantic water and plankton onto the shelf at least as far south as Icy Cape (Ladd et al., 2016; Pinchuk et al., 2017). Direct measurements of these kinds of variations, however, are limited to a few locations and mostly of relatively short (a few days) duration.

Danielson et al. (2014) addressed the limited scope of direct long-term measurements by using a combination of atmospheric reanalyses, oceanographic observations, and numerical ocean model experiments to investigate the circulation of the northern Bering Sea shelf and Chukchi Sea shelf. They found that the transport in Bering Strait was influenced not just by local winds, but also by larger-scale atmospheric patterns, particularly the longitudinal position of the Aleutian Low. Variations on synoptic time scales of a few days can also be related to coastally-trapped waves that are remotely generated. They also found that large-scale atmospheric patterns influence the ocean in both the Pacific and the Arctic, ultimately impacting the strength of the pressure head between the Pacific and Arctic Oceans. Danielson et al. (2014), and references therein, represent a good resource for readers interested in delving into the progress that has been made in understanding the physical oceanography of the Chukchi Sea and its controls.

The biology of the Chukchi Sea has also received prior attention. Most recently, several special issues are of note: collections of papers on the ecology of the northeastern Chukchi Sea (Hopcroft and Day, 2013; Dunton et al., 2014), the Russian-American Long-term Census of the Arctic (Crane and Ostrovskiy, 2015) and the first SOAR special issue (Moore and Stabeno, 2015). As discussed by Day et al. (2013), the Chukchi Sea features contrasting ecosystems in close proximity that are related to water masses of different origin. Three water masses enter the Chukchi from the Bering Sea: salty, nutrient-rich Anadyr Water; the slightly fresher, nutrient-rich Bering Shelf Water; and the warmer and fresher still Alaskan Coastal Water. Anadyr Water and Bering Shelf Water tend to include higher zooplankton biomasses (Springer et al. 1989) and are particularly important in structuring the largest area of the Chukchi Sea shelf. As indicated in Pisareva et al. (2015), among others, the lateral distributions of the water masses of the region vary with the winds. Physical oceanographic fluctuations on interannual time scales have been found to be prominent forcing functions within the ecosystem from lower-trophic levels (e.g. Questel et al., 2013; Busby et al., 2015; Ershova et al., 2015; Pinchuk and Eisner, 2017) to intermediate levels (Sigler et al., 2017) and on to top predators (e.g., Aerts et al., 2013; Gall et al., 2016). The overall warming of the region and the associated longer ice-free season (Grebmeier et al., 2015; Overland and Wang, 2010; Wood et al., 2015) should be having a tangible effect on the ecosystem of the

Chukchi Sea. This raises a question: Are systematic and long-term changes in the physical oceanography of the Chukchi Sea emerging above the year-to-year variations?

This paper describes the mean and variability in the physical oceanography of the Chukchi Sea during the months of June through October across a 36-year period. We focus on the warm months with limited (or no) ice cover, because it is a critical period in this arctic marine ecosystem. It is a time of year when the poleward advection through Bering Strait is enhanced and there is increasing production at lower-trophic levels, which provides critical nutrition for marine mammals and seabirds (e.g. Grebmeier et al., 2015; Kuletz et al., 2015; Citta et al., 2015). Our analysis is based on monthly mean gridded data from the operational ocean analysis system 4 (Ocean-S4) developed by the European Centre for Medium-Range Weather Forecasts (ECMWF). Specifically, we use this system's reanalysis product (ORAS4) for the years of 1979 through 2014, with a focus on vertically-integrated currents and heat contents. Our findings include descriptions of the seasonal evolution of the mean flow and heat content, and of the long-term trends in heat content. We characterize the variability in the flow in terms of five patterns determined from a cluster analysis of anomalous SSH distributions. We conclude with a summary and discussion of possible connections between our physical oceanographic results and the marine ecosystem. Our overarching goal is to provide context for future marine research focused on the Chukchi Sea region, in particular how fluctuations in the flow described here may be useful in the further development of the Arctic Marine Pulses (AMP) model (Moore et al., 2017, this issue).

2. Data sources and methods

Our analysis is based on monthly mean oceanographic data from the ORAS4 operational ocean reanalysis that is produced by the European Centre for Medium-Range Weather Forecasts (ECMWF). This product is based on output from Nucleus for European Modeling of the Ocean (NEMO) numerical ocean model simulations constrained by observations via the NEMOVAR ocean data assimilation system. The observations assimilated include sea surface temperature (SST) and sea-ice products, temperature and salinity profiles, and SSHs estimated from altimeters (the latter from October 1992 onward). The atmospheric forcing, i.e. the surface fluxes at the air-sea interface, is derived from atmospheric reanalyses, specifically ECMWF's ERA-40, ERA-Interim, and operational archives. The surface fluxes are adjusted by nudging to observed SST and sea-ice concentration fields. Errors that are potentially introduced by this procedure of a compensating nature in the region of interest are unknown. Balmaseda et al. (2013) provide an overview of ORAS4, including an evaluation of some of its output with independent observations. The ORAS4 data we used were downloaded from a web site maintained by the Asia-Pacific Data-Research Center of the University of Hawaii at the following address: http://apdrc.soest.hawaii.edu/data/data.php. We note that the ORAS4 product was just recently extended back to 1958, and forward through 2015; users are advised that the first two decades of data in the new version include large uncertainties and should be used with caution.

We recognize that the introduction of SSH data in 1992 could compromise the ORAS4 product through the creation of artificial trends or biases. We addressed this concern in two ways: (1) by comparing ORAS4 output with that from the Simple Ocean Data

Assimilation (SODA) version 2.2.4 (Giese and Ray, 2011), an ocean reanalysis that does not include SSH data in its assimilation procedure; and (2) by repeating a portion of our analysis for just the years of 1993 through 2014, and comparing the results with those from the years of 1979 through 2014 of the full data set.

We emphasize that our analysis focuses on the broad-scale aspects of the flow in the Chukchi Sea during June through October. The backbone of ORAS4 is the NEMO numerical ocean model, which has horizontal resolution of 1 degree outside of the tropics. An important implication is that this product is not appropriate for specifying details in the flow in the immediate vicinity of the coast or prominent bathymetric features. Our objective is to use it to describe the seasonal mean evolution of the physical oceanography of the Chukchi Sea on 100+ km length scales and in terms of vertically-integrated currents and heat content during the June through October period, and to explore the variability in these conditions from 1979 to 2014. For these purposes, we expect oceanographic fields from ORAS4 are especially valuable for the western part of the Chukchi Sea in Russian waters, where publicly available oceanographic observations (aside from SST) are limited.

The variability in physical oceanographic conditions during the period of 1979–2014 is examined here using distributions of SSH as the discriminatory variable. The distribution of SSH reflects the barotropic component of the flow, which dominates monthly mean transports in the Chukchi Sea, because it is relatively shallow (generally < 60 m). Our method employs cluster analysis (e.g. Gordon, 1981) to identify basic patterns in SSH and the temporal variability in these patterns over the period considered. Specifically, we use the non-hierarchical and relatively simple technique of k-means clustering. In a nutshell, this technique separates the individual realizations, in our case monthly mean SSH anomaly distributions, into a specified number of clusters, with each member belonging to the cluster that minimizes the distance of the data points from their mean counterparts for that cluster.

Our method is not designed to yield necessarily the most dynamically relevant modes, but rather a reduced set of common patterns amenable to further investigation. Principal component analysis (PCA) has also been used for this kind of purpose. We are not claiming that k-means clustering is superior in all aspects, but in contrast to PCA, it does not require that the modes be orthogonal to one another, nor that field distributions occur in spatial patterns of opposite polarity. A paper by Robertson and Ghil (1999) represents a previous example of the use of k-means clustering to characterize weather regimes.

The steps used in forming the clusters are as follows. Monthly mean values of SSH were determined for each of the 74 grid points within our Chukchi Sea shelf region of interest (see Fig. 1 for areal boundary). Mean SSH anomalies for each of these grid points were then computed for the months of June through October for each of the years of 1979 through 2014: a total of 180 realizations. A series of experiments were conducted with different values for k, the number of clusters. We examined the spatial patterns in the composite SSH anomaly distributions for each cluster category. Similar (i.e. recurring) patterns emerged using k values greater than four, and the particular months that were included in a single cluster category were generally consistent. With the twin goals of simplicity and completeness in characterizing the fluctuations, we settled on a value of k = 5. It should be noted that the ordering of the clusters depends on initial (seed) values for the centers of each cluster that are chosen randomly, and then corrected by an iterative procedure. Hence, the ordering of the clusters does not relate to the proportion of variance explained, unlike the modes from PCA. Again, we are only contending that our method serves as one way to characterize the variability in the monthly mean flow in the region of interest, but it does appear to yield reasonable and informative results, as will be shown below.

3. Results and Discussion

3.1 Mean flow and heat content

We begin by summarizing the mean flow from June through October. A map of the mean distribution of SSH, and the vertically integrated flow in vector form, from ORAS4 for the years 1979–2014 is shown in Fig. 2. As found in previous studies, the mean flow on the Chukchi Shelf is northward, with stronger east-west gradients in SSH and, hence, higher velocities in the eastern portion of the domain. There is a weak signature of the northeast flow of the Alaskan Coastal Current (ACC) described by Paquette and Bourke (1974), and enhanced northward flows through Herald Valley and the Central Channel (Weingartner et al., 2005). Nevertheless, the horizontal resolution of the reanalysis is too coarse to resolve the known details in the flow (Weingartner et al., 2013) in the vicinity of mesoscale bathymetric features of the northeastern Chukchi Sea shelf. The ORAS4 better serves to describe the variability in the broad-scale (100+ km) flow, which is the primary objective of this study. For example, it is appropriate for examining fluctuations in the overall flow in the western Chukchi Sea along the Siberian coast. This region has relatively weak northwestward currents in the mean (Fig. 2), but as will be shown below, this mean is composed of months of strong northwestward flow, relatively quiescent conditions, and occasional sustained southeastward flow, i.e., a prominent SCC.

Bering Strait represents the primary source of water for the Chukchi Sea, and the mean and variability in this source from the ORAS4 product was considered. Mean values of the northward currents at 66.5°N averaged from 168.5 to 167°W were ~25 cm s^{-1} in early summer and ~15 cm s^{-1} in winter, with substantially greater year-to-year variability in winter months. These mean values are comparable, but smaller, than those reported by Danielson et al. (2014) for the A3 mooring at 66.3°N, 169.0°W. This discrepancy may be related in part to the coarse spatial resolution of the ORAS4 reanalysis and hence its misrepresentation of the details in the flow immediately to the north of Bering Strait. In terms of interannual variations, Woodgate et al. (2015) show that relatively weak Bering Strait transports occurred in 2001, 2005 and 2012 and that strong transports occurred in 2004, 2007, 2011 and 2013. In accordance with this finding, the mean northward currents from ORAS4 were below the mean in 2001, 2005 and 2012, and above the mean in 2004, 2007 and 2011, with deviations from the mean of about 20-35%. An exception is represented by 2013, which featured a relatively high mean transport in the observations but had near normal mean currents in ORAS4. Overall, it appears that ORAS4 represents the mass transport of water through Bering Strait into the Chukchi Sea reasonably well.

Next we consider the evolution of oceanographic conditions in the Chukchi Sea from June through October by examining monthly mean vertically integrated temperatures and currents for the years 1979-2014 (Fig. 3). The strength of the poleward flow is generally greater in the earlier months (June and July) than in the later months (September and October). Similar results are found in the observations for Bering Strait (Woodgate et al., 2005) and at Icy Cape (Stabeno et al., 2017). On the other hand, the basic structure of the mean flow is similar in all five months, which allows them to be treated as a single group in the cluster analysis. With regard to the temperature distribution, the meridional gradients are particularly strong from July through September, with the zone of peak gradients moving from south to north (with the melting of sea ice). The eastern portion of the Chukchi Sea is generally warmer than the western portion, reflecting the enhanced flow of relatively warm water associated with the ACC.

In more quantitative terms, what controls the seasonal evolution of heat content in the Chukchi Sea? To address that question, we evaluated the mean contributions of horizontal advection ($UT_x + VT_y$) and net surface heat fluxes to the vertically integrated heat content during the months of June through October (Fig. 4). Our analysis domain here does not extend as far south toward Bering Strait as in our earlier analysis. The strong flow in the vicinity of Bering Strait combined with small errors in specification of the direction of the current relative to the orientation of the isotherms lead to unrealistically large values for the advective term. This limitation of the one-degree grid spacing for the temperature and velocity fields used in the present analysis appears to be minimal for the portion of the Chukchi Sea north of about 67°N. Both the advective and surface flux terms are generally stronger in the southern than in the northern portion of the Chukchi during June and July. Horizontal advection is largely responsible for the continued heating from August into September. The surface heat flux changed sign from heating the water column during August to cooling it during September. Because of the continuous (in the mean) poleward transport of relatively warm water, the surface and advective fluxes are counteracting each other late into the warm season. The surface and advective fluxes are both warming terms in the heat budget early in the warm season, with the melting of sea ice cooling the water column at rates of roughly 1-2 °C per month in June (relatively little ice is present afterwards).

3.2 Temporal variability and trends

Next we focus on the temporal variability in heat content in various parts of the Chukchi Sea. For this purpose we considered time series of spatially averaged temperatures in three different sub-regions (Fig. 1), given the potential for meaningful spatial variations in trends. The three regions selected are: (1) a southern area (67–68°N, 172–165°W) at the southern end of the Hope Sea Valley, which is expected to be most sensitive to flow through Bering Strait; (2) a northeastern area (70–71.5°N, 168–162°W) between Herald Shoal and Hanna Shoal, which is likely to primarily reflect the variability in ACC (Stabeno et al., 2018); and (3) a northwestern area (69.5–71°N, 177–171°W) including a region of relatively deep (>50 m) water south of Herald Canyon, which should serve as an indicator of thermal conditions in the western Chukchi Sea. Averages were computed separately for June–July (Fig. 5a) and for September–October (Fig. 5b) to assess possible differences between the early and late portions of the warm season. As expected, on average the south is warmer than either of the northern regions, especially early in the warm season. For the period of 1979–2014, the greatest overall warming was in the northeastern area (~1.8 °C) and the least overall warming was in the southern area

(~0.9 °C). Considering both times of year, and the three locations as a group, the warming from 1979 through 1996 was about five times stronger than that from 1997 through 2014. Positive trends significantly different from zero at the 90% confidence level were found for June-July at the southern location, and for September-October at the northeastern and southern locations. The second half of the record lacked trends that were significantly different from zero ($p < 0.10$). There were greater positive correlations in the interannual variations between early (June–July) and late (September–October) temperatures in the northeastern and northwestern areas ($r \sim 0.7$) than in the southern area ($r \sim 0.55$). The latter result probably reflects the greater ventilation rate in the south related to its strong mean currents.

The lack of prominent warming in the second half of the record was not anticipated. Due to the concern mentioned in the methods section about the possibility of artifacts introduced by the assimilation of SSH data beginning partway through the record, we also examined the heat content in the SODAv2.2.4, which is not subject to this step change in data availability in 1992. Specifically, we examined the heat content at the end of the warm season (September-October averages) in the northeastern Chukchi Sea. There is a close correspondence between the two different reanalysis products in terms of their identification of individual warm and cold years. Both products indicate a warming of about 2°C from the early 1980s to late 1990s, and a lack of statistically significant trends afterwards.

Next we consider the temporal variability in the currents, focusing on the along-shore component of the current at two coastal locations, and the meridional currents in Herald Canyon to the east of Wrangel Island (measurement locations indicated as asterisks in

Fig. 1). The along-coast component of the flow at a northeast location off the coast of Alaska near Icy Cape (Fig. 6a) indicates exclusively northeastward-directed flow early in the warm season (June–August). More variable flow is found in September and especially October. There are negative trends in this flow for each of the months considered, with the magnitudes for June and August being significant at the 90% confidence level. Negative values, which signify reversals to southwestward flow, occur intermittently through the entire record, with reversals of larger magnitude occurring in the second half. The net weakening of the ACC found here (with considerable sub-seasonal and interannual variability) is consistent with the lack of warming in the second half of the record. A southwest location at the Siberian coast (Fig. 6b) experienced a preponderance of negative (implying west-northwestward) along-shore currents with positive values, i.e. strong manifestations of the SCC, occurring mostly during the latter portion of the warm season. More specifically, 13 of the 18 Octobers during the second half of the record had flow toward the east-southeast, while only 6 out of 18 Octobers during the first half of the record had an along-coast component of the flow in this direction. The overall trend in the flow for October is marginally significant ($p \sim 0.17$). Net changes of a similar sense, but with weaker magnitudes, were found for the months of July through September. The meridional flow at the northwest location in Herald Canyon is shown in Figure 6c. There is a tendency for less poleward flow in each month. The trends for June, September and October are significantly different from zero at the 90% confidence level, with greater net changes during September and October. The only two months with net southward flow were August 2011 and September 2012. More information on how the nature of the flow has changed over the period of record is provided in the following section.

3.3 Flow patterns identified by cluster analysis

Here we depict the flow patterns characteristic of each cluster type, and the temporal variability of occurrence for each cluster type. We begin by presenting the distributions of the composite SSH anomaly and mean vertically-averaged currents (not anomalies) with each of the five cluster types. As mentioned in Section 2, the ordering of the clusters is arbitrary.

Cluster 1 (Fig. 7a) represents a relatively low amplitude pattern with weak southeastward flow anomalies in the western Chukchi (due to anomalously higher SSH along the Siberian coast) and a slightly suppressed ACC relative to the mean (Fig. 2) in the eastern Chukchi Sea. Cluster 2 (Fig. 7b) features a stronger than normal ACC concentrated near the coast and weak northwestward flow anomalies in western Chukchi Sea. The primary signatures of Cluster 3 (Fig. 7c) are strong anomalous flow from west to east across the northern Chukchi Sea, a weak southeastward SCC in the mean, and a weaker than normal flow to the north out of Bering Strait. Cluster 4 (Fig. 7d) is distinguished by a strongly suppressed ACC with almost zero mean currents near Icy Cape; its pattern is close to a mirror image of the pattern with Cluster 2. The attributes of Cluster 5 (Fig. 7e) include moderate flow anomalies from east to west across the northern Chukchi Sea, strong northwestward flow along the Siberian coast, poleward transport anomalies through Bering Strait, and a broad flow instead of a coastally confined ACC. This pattern resembles that of Cluster 3 for the entire Chukchi Sea, but of opposite sign.

Clusters 1 and 2 occur most often (25% and 24% of the months, respectively) and Cluster 3 occurs least often (12% of the months). Information about the timing of the realizations of the individual cluster members will be presented later in this section.

Some basic statistics were applied to determine how well the SSH anomaly distributions for the months comprising each cluster type correspond with the composite pattern for that type. The average spatial correlation coefficient between the SSH anomaly distribution for an individual month with the composite for its type was ~0.66. Lower spatial correlations were typical for the months in Cluster 1, which is consistent with it being a low amplitude pattern. The root mean square difference between the SSH anomaly values during an individual month and the composite SSH anomaly, averaged across all the grid points, ranged from about 0.035 to 0.040 m, which is about one-half of the average standard deviation in SSH. By this measure, Clusters 3 and 5 had greater deviations among the individual cluster members, which is expected since they are relatively high amplitude patterns.

We explored whether the discontinuity in the altimetry data for assimilation may have impacted the characteristic patterns in SSH variability. Our approach was to carry out an additional cluster analysis for just the period of 1993-2014 that included altimetry data for ORAS4 input, and compare the results with that from the full data set of 1979-2014. For the overlapping 22 years (110 separate months), there were five months that were assigned to different cluster categories. The primary change was that Cluster 3 lost four of its lower-amplitude members to Cluster 1 in the cluster analysis using the shorter (1993-2014) data set. The implication is that the step change in the altimetry data used for the ORAS4 reanalysis appears to have had minimal influence on the categorization of the characteristic patterns of SSH variability.

A close correspondence was found between the regional atmospheric forcing during the months comprising each cluster type and the composite SSH anomaly distributions described above. Here we summarize the atmospheric forcing with composite sea level pressure (SLP) anomaly maps; such maps can be used to deduce the barotropic forcing of the ocean. The SLP pattern for Cluster 1 (Fig. 8a) implies anomalous winds from west to southwest and associated Ekman transports to the southeast in the western Chukchi, and little net effect on the flow in the eastern Chukchi Sea. The anomalous SLP for Cluster 2 (Fig. 8b) implies southerly wind anomalies and, hence, a set-up favorable for an enhanced ACC as indicated in the corresponding SSH field. The enhanced north-south SLP gradient for Cluster 3 (Fig. 8c) indicates strong westerly wind anomalies and southward Ekman transports. The distribution of anomalous SLP during the months in Cluster 4 (Fig. 8d) is consistent with a suppressed ACC and only modest effects on the flow in the western Chukchi Sea. The SLP pattern for Cluster 5 (Fig. 8e) is almost exactly opposite to that for Cluster 3, as also found for the SSH distributions for the two clusters. The SLP distribution for Cluster 5 indicates anomalous winds from the east-northeast; the accompanying northwestward flow anomalies in the western Chukchi for this cluster are consistent with the results from a numerical model in conditions of prescribed east winds (Winsor and Chapman, 2004)

Summary statistics on the occurrence of each cluster type by month are presented in Table 1, with separate totals for the first and second halves of the 36-year record. Figure 9 affords a complementary perspective on the cluster type for each of the five months during the years 1979 through 2014. The SSH pattern associated with Cluster 1 occurs more frequently in June, July, and August as compared to September and October (Table 1). Cluster types 2 and 4 tend to occur more often from July through September than in June or October, but only to a marginal extent. Cluster 3 flow tends to occur more often in June and October than the other months. Only Clusters 1 and 4 had a notably different frequency of occurrence in the first half versus the second half of the record. Cluster 1-type flow occurred more often during the first half of the record; after 2000, it did not occur at all during the months of September and October. Cluster 4-type flow was more frequent in the second half of the 36-year record during the months of August through October. Since Cluster 4 is associated with relatively weak poleward transports in the southern Chukchi Sea and a suppressed ACC, the greater frequency of its occurrence is consistent with a lack of warming in the second half of the record, especially for the months of September and October.

Our cluster analysis provides a means for assessing the persistence of various flow regimes in the Chukchi Sea within each June-October period. There were 27 cases of 2 months in a row in the same SSH cluster type, and 4 cases of 3 consecutive months of a particular cluster type; hence, 66 of the 180 months considered are within a multi-month regime. This is close to what would be expected from chance, given that there are 4 (3) opportunities each year for 2 (3) months in a row in a particular flow category. These results imply the dominance of month-to-month variations in the flow versus seasonal anomalies in the Chukchi Sea. We note that our analysis does not address the character of the interannual variability, but our inspection of the time series of the occurrences of each cluster type, as illustrated in Fig. 9, suggest a lack of sustained flow regimes.

Currents have been measured by moorings along a cross-shore oriented transect at Icy

Cape since August 2010 (Stabeno et al., 2017), providing the opportunity to compare the present results with direct data. To begin with, these observations have revealed that the flow at Icy Cape typically includes a branch of eastward flowing Central Channel water joining the northeastward flowing ACC, which exits the shelf via Barrow Canyon. This onshelf-directed flow is evident in the SSH patterns of Cluster types 1, 3, and 4 (Fig. 7). Along-coast transports were estimated at Icy Cape for each month that moorings were deployed. The measured monthly transports anomalies associated with Clusters 1–3 are positive (northeastward), with an average magnitude of 0.2 Sv. The six months of the data set designated here in Cluster 4 had the weakest measured ACC on average. The monthly mean transport anomalies during these months were all negative (southwestward flow) with a mean of -0.2 Sv. The composite SSH anomaly pattern with Cluster 5 indicates westward flow anomalies offshore of Icy Cape, and the months of this type should tend to include reduced contributions of Central Channel water to the ACC. Thus, it is not surprising the monthly mean observed transports associated with Cluster 5 are also negative (~0.1 Sv), with considerable variability among the five months of this type. The strongest negative transport (-0.5 Sv) measured at Icy Cape occurred in October 2010, which is consistent with the large negative anomaly for that month from ORAS4 shown in Figure 6a. In general, the Icy Cape mooring observations are consistent with the currents from ORAS4 and the results from our cluster analysis.

Danielson et al. (2016) represents another opportunity to compare our results with observations. They analyzed physical oceanographic conditions and nutrient and phytoplankton concentrations in the eastern Chukchi Sea from August 7 – September 24 in 2012 and 2013. During 2012, there was a change from a relatively strong ACC in

August to weaker mean flow in September. This is consistent with our cluster analysis, which indicates that September 2012 is in Cluster 4, which has a composite SSH pattern featuring a suppressed ACC. For 2013, Danielson et al. (2016) report a weak ACC during August, and northwestward flow during September. Again, this compares favorably with our results, which indicate the months of August and September in the Cluster 4 and 5 categories, respectively.

We close our review of the results from the cluster analysis with material on the mean upper-ocean (surface to a depth of 20 m) horizontal divergence associated with each cluster type, in terms of anomaly maps (deviations from the distribution of divergence in the mean). It bears reiterating that the relatively coarse resolution ORAS4 reanalysis is ill-suited for specifying smaller-scale features such as in the immediate vicinity of the coast or in the southern portion of the region of interest near Bering Strait. On the other hand, we posit that the broad (100+ km) patterns in anomalous divergence over the central Chukchi Sea may be reasonably reliable. If so, they are relevant, from a biological point of view, in that divergence implies upwelling, which can be important for the supply of nutrients from below to the euphotic zone especially late in the summer when there is less sunlight, and convergence may serve to concentrate zooplankton and other prey for planktivorous fishes, seabirds and marine mammals. Concerning the magnitudes of this effect, the contour interval of 2×10^{-8} s^{-1} in the anomaly maps of Figs. 10a-e is equivalent to a vertical velocity at a depth of 20 m of about 1 m per month. In general, the anomalies in horizontal divergence for each cluster type are weak relative to the divergence in the mean, which is illustrated in the lower-right corner of Fig. 10. Presumably, the mean divergence pattern primarily reflects the effects of the bathymetry, while the anomaly patterns (Figs. 10a-e) show how and when the perturbations in the flow with each cluster type are manifested.

The mean divergence during the months in Cluster 1 (Fig. 10a) is a relatively low-amplitude anomaly pattern with small areas of moderate convergence south of Wrangel Island and north of Barrow, and mostly weak divergence across much of the central Chukchi Sea. The divergence signal in Cluster 2 situations (Fig. 10b) is concentrated in the eastern part of the Chukchi Sea, with convergence along the coast in the vicinity of Cape Lisburne and divergence offshore. The months in Cluster 3 tend to feature relatively strong convergence along the Siberian coast and divergence along the western coast of Alaska (Fig. 10c). This distribution is consistent with the Ekman transports toward the Siberian coast mentioned above, and a bifurcation in the anomalous flow approaching the Alaskan coast, namely a suppression of the northward flow in the southern portion of the ACC (Fig. 6c). The divergence anomaly pattern for Cluster 4 (Fig. 10d) is essentially opposite to that of Cluster 2, with mostly convergence in the central and northern Chukchi Sea. This is consistent with the anomalous SSH pattern for Cluster 4, which is basically the reverse of that for Cluster 2 in the central and eastern part of the domain. Similarly, the anomaly pattern with Cluster 5 (Fig. 10e) is mostly opposite to that of Cluster 3, with divergence off the Siberian coast and mostly convergence off the coast of Alaska. An exception is just north of Cape Lisburne, where there is divergence in the composites for both Cluster 3 and Cluster 5.

4. Summary and Ecosystem Implications

The objective of this study was to document physical oceanographic conditions that have occurred on the Chukchi Sea shelf during the June through October period for the years of 1979–2014. The ORAS4 ocean reanalysis, which consists of output from simulations using a numerical ocean model constrained by observations, was used for this purpose. Since this information is limited to monthly means on a one-degree grid, our focus has been on broad-scale aspects of the flow. Our findings represent a long-term physical context for the biological studies included in this special issue and for future arctic ecosystem research on biophysical relationships.

The record of vertically integrated temperatures on the Chukchi shelf revealed a great deal of year-to-year variability, as expected, but also an unanticipated result in terms of longer-term trends. In particular, minimal warming occurred over the last half of the 36-year period of analysis, especially in September and October. This was unanticipated in light of the overall warming of the Arctic and decline in sea-ice extent at the end of the melt season. During this same time period, spring arctic sea-ice extent over the entire Arctic Ocean and marginal seas has decreased by an average of 2.6% per decade (http://nsidc.org/arcticseaicenews/). The lack of warming on the Chukchi shelf during this time of year may be related to changes in the flow, which tended to be less poleward near Herald Canyon and along the northwest coast of Alaska near Icy Cape, as compared with the first half of the analysis period. In other words, there appears to have been a slight decrease in the advection of warm Bering Sea waters since about the turn of the century. The monthly mean currents also appear slightly more variable in September and October during the second half of the record.

The gridded data set from ORAS4 is amenable to diagnosis of the patterns of variability and for this purpose, we implemented a k-means cluster analysis of SSH anomaly distributions. The 180 months were separated into five cluster categories; we focused on composites formed from the months comprising each category. The first category, termed Cluster type 1, is a lower-amplitude pattern. It occurred during 31% of the months in the first half, but only 19% of the months in the second half of the record. It did not occur at all in September or October after 2000, which is consistent with the slightly greater variability seen in the currents mentioned above.

Cluster types 2 and 4 reflect SSH distributions associated with enhanced and suppressed poleward flow with the ACC, respectively. The emergence of SSH anomaly patterns of this character was expected since previous observational studies have found sizable fluctuations, and even reversals, in the ACC. The cluster analysis categorized 44 months in Cluster type 2 and 33 months in Cluster type 4, suggesting the potential for skewness in the temporal variability of the ACC during the warm months. There did not appear to be a difference in the occurrence of these patterns between the first and second halves of this time series.

Cluster types 3 and 5 are virtually mirror images of one another and suggest a mode of variability for the Chukchi Sea shelf that may not have been previously appreciated. These two cluster types have strong expressions in the northwestern portion of the Chukchi Sea, where the mean flow is weak, but the variability is substantial. Cluster 3 type flow, which occurs less often than the rest of the cluster types, features southeastward flow over a broad region extending from the Siberian coast to past Wrangel Island. The composite pattern associated with Cluster 5 includes stronger than normal flow through Bering Strait, with a disproportionate portion of this flow not joining the ACC but rather flowing northwest toward and beyond Wrangel Island, which is the region that experiences southeastward flow during Cluster 3 months. This difference may have important biological consequences. Planktonic organisms originating in Hope Valley are apt to undergo considerably different trajectories in Cluster 3 versus Cluster 5 flow regimes, with life history implications. Similarly, Cluster 3 may indicate a mode that transports Eastern Siberian Sea plankton into the eastern Chukchi Sea. The high month-to-month variability observed in cluster type helps to explain why short-term field studies indicate a range of outcomes, even in the same year.

The long-term and broad-scale oceanography described in this paper provides background information for related physical and biological oceanography studies, and potentially aids in the interpretation of ecosystem observations. For example, Hill et al. (this issue) explore decadal trends in regional primary production, including the onset of under-ice phytoplankton blooms. Results from the cluster analysis described here may shed additional light on their interpretations or promote avenues for further research. Support for this contention is provided by the consistency between the northward transports through Bering Strait found by Danielson et al. (2016) and the results from our cluster analysis for 2012 and 2013, and ultimately the differences in nutrient concentrations and chlorophyll standing stocks between the two years. Similarly, results from our cluster analysis may provide additional context for the formation and transport of corrosive water (Cross et al., this issue) and with regards to the deposition patterns of surface sediments on the Chukchi shelf (Cooper and Grebmeier, this issue).

At a much broader scale our paper supports the further development of the Arctic Marine Pulses (AMP) model, linking regional biological processes with seasonal and annual variability in the physical environment (Moore et al., this issue). Specifically, the AMP model aims to encourage integrated research to track seasonal sea-ice and current-flow dynamics, coincident with variability in nutrients, benthic and pelagic production. For example, Hope Valley and the northeast Chukchi Sea feature comparatively high lower-trophic level production (based on sampling at Distributed Biological Observatory stations), and perhaps fluctuations in the flow— as revealed in the type of analysis used here— are key aspects of their ecosystems.

Beyond this special issue, our work extends the frame of past physical oceanographic studies of the Chukchi Sea, and can supplement the interpretation of arctic biological and ecosystem studies across time and space. For example, the review and analysis of long-term changes in the zooplankton community of the Chukchi Sea by Ershova et al. (2015) documents both interannual variability and long-term trends, and explores links to contrasting water masses. Other works also demonstrate the connection between plankton community composition and currents for zooplankton as well as larval fish (e.g. Norcross et al., 2010; Pinchuk and Eisner, 2017). Gall et al. (2016) connects changes in available prey to trends in Chukchi Sea marine bird populations, within a context of variable flow through the Bering Strait and changes in the Chukchi Sea physical environment. From a holistic perspective, changes in oceanographic conditions can lead to species replacements or distributional shifts that disrupt entire food webs. For example, many arctic species prey on arctic cod (*Boreogadus saida)* (e.g. Whitehouse et al., 2014), and benefit from the high lipid content of that fish and the efficiency at which it converts its prey to fish biomass at very low temperatures (Copeman et al., 2016; Laurel et al., 2016). Saffron cod (*Eleginus gracilis*) have the potential to replace arctic cod in the warming coastal areas of the Beaufort and Chukchi Seas and this could impact the nutrition available to higher trophic levels (Copeman et al., 2016; Laurel et al., 2016). Oceanographic conditions from reanalyses, such as presented here, provide a means for better understanding past biological observations, especially their potential linkages to the physical environment. The type of analysis we conducted may also be useful in comparing regions such as the Chukchi and Barents Seas (Hunt et al., 2013; Logerwell et al., 2015).

Finally, it would be interesting to determine whether the characteristics of the temporal and spatial variability diagnosed here are replicated by global climate models. Historical simulations for recent decades in forecast mode, i.e., not constrained by observations, would be appropriate for this purpose. It would also be worthwhile to explore how the nature and frequency of patterns in present-day simulations compare with their counterparts for later in the 21st century.

Acknowledgments

We appreciate helpful discussions with Sue Moore, Tom Van Pelt and Kevin Wood. This study is part of the Synthesis of Arctic Research (SOAR) and was funded in part by the U.S. Department of the Interior, Bureau of Ocean Energy Management, Environmental Studies Program through Interagency Agreement No. M11PG00034 with the U.S. Department of Commerce, National Oceanic and Atmospheric Administration (NOAA), Office of Oceanic and Atmospheric Research (OAR), Pacific Marine Environmental Laboratory (PMEL). This publication is [partially] funded by the Joint Institute for the

Study of the Atmosphere and Ocean (JISAO) under NOAA Cooperative Agreement NA10OAR4320148 (2010-2015) and NA15OAR4320063 (2015-2020), Contribution No. 2016-01-42. This publication is contribution EcoFOCI-0879 to NOAA's Ecosystems and Fisheries-Oceanography Coordinated Investigations and PMEL Contribution No. 4575.

References

Aagaard, K., Weingartner, T.J., Danielson, S.L., Woodgate, R.A., Johnson, G.C., Whitledge, T.E., 2006. Some controls on flow and salinity in Bering Strait. Geophys. Res. Lett. 33, L19602.

Aerts, L.A.M., Kirk, A., Lomac-MacNair, K., McFarland, A., Watts, B., Seiser, P., Brueggeman, J., Wisdom, S., Schudel, C., 2013. Marine mammal distribution and abundance in the offshore northeastern Chukchi Sea during the open water season. Cont. Shelf Res. 67, 116–126.

Balmaseda, M.A., Mogensen, K., Weaver, A., 2013. Evaluation of the ECMWF ocean reanalysis system ORAS4. Q.J.R. Meteorol. Soc. 139, 1132–1161, doi:10.1002/qj.2063.

Busby, M.S., Duffy-Anderson, J.T., Mier, K.L., Tabisola, H.M., 2015. Ichthyoplankton assemblages and distribution in the Chukchi and Northern Bering Seas 2012–2013. US Dept. of the Interior, Bureau of Ocean Energy Management, Alaska OCS Region. OCS Study BOEM 2011-AK-11-08 a/b. 38 pp.

Citta, J. J., et al. 2015. Ecological characteristics of core-use areas used by Bering-Chukchi-Beaufort (BCB) bowhead whales, 2006–2012, *Prog. Oceanogr., 136,* 201–222, doi:10.1016/j.pocean.2014.08.012.

Cooper, L.W., Grebmeier, J.M. this issue. Deposition patterns on the Chukchi Shelf using radionuclide inventories in relation to surface sediment characteristics.

Cross, J.N., Mathis, J.T., Pickart, R.S., Bates, N.R. this issue. Formation and transport of corrosive water in the Pacific Arctic region.

Crane, K., Ostrovskiy, A., 2015. Introduction to the special issue: Russian-American Long-term Census of the Arctic (RUSALCA). Oceanography 28(3), 18–23, doi:10.5670/oceanog.2015.54.

Copeman, L.A., Laurel, B.J., Boswell, K.M., Sremba, A.L., Klinck, K., Heintz, R.A., Vollenweider, J.J., Helser, T.E., Spencer, M.L. 2010. Ontogenetic and spatial variability in trophic biomarkers of juvenile saffron cod (Eleginus gracilis) from the Beaufort, Chukchi, and Bering Seas. Polar Biology 39:1109-1126.

Danielson, S.L., Weingartner, T.J., Hedstrom, K.S., Aagaard, K., Woodgate, R., Curchitser, E., Stabeno, P., 2014. Coupled wind-forced controls of the Bering-Chukchi shelf circulation and the Bering Strait throughflow: Ekman transport, continental shelf waves, and variations of the Pacific-Arctic sea surface height gradient. Prog. Oceanogr. 125, 40–61, doi:10.1016/j.pocean.2014.04.006.

Danielson, S.L., L. Eisner, C. Ladd, C. Mordy, L. Sousa, and T.J. Weingartner, 2016. A comparison between late summer 2012 and 2013 water masses, macronutrients, and phytoplankton standing crops in the northern Bering and Chukchi seas. Deep-Sea Res. II, doi: 10.1016/j.dsr2.2016.05.024.

Day, R.H., Weingartner, T.J., Hopcroft, R.R., Aerts, L.A.M., Blanchard, A.L., Gall, A.E., Gallaway, B.J., Hannay, D.E., Holladay, B.A., Mathis, J.T., Norcross, B.L., Questel, J.M., Wisdom, S.S., 2013. The offshore northeastern Chukchi Sea, Alaska: a complex high-latitude ecosystem. Cont. Shelf Res. 67, 147–165.

Dunton, K.H., J.M. Grebmeier, J.H. Trefry, 2014. The benthic ecosystem of the northeastern Chukchi Sea: An overview of its unique biogeochemical and biological characteristics. Deep-Sea Res. II 102: 1-8

Ershova, E.A., Hopcroft, R.R., Kosobokova, K.N., Matsuno, K., Nelson, R.J., Yamaguchi, A., Eisner, L.B., 2015. Long-term changes in summer zooplankton communities of the western Chukchi Sea, 1945–2012. Oceanography 28(3), 100–115.

Gall, A.E., Morgan, T.C., Day, R.H., Kuletz, K.J., 2016. Ecological shift from piscivorous to planktivorous seabirds in the Chukchi Sea, 1975–2012. Polar Biol., doi:10.1007/s00300-016-1924-z.

Gong, D. and Pickart, R.S., 2015. Summertime circulation in the eastern Chukchi Sea. *Deep-Sea Research II* 105, 53-73.

Gordon, A.D., 1981. Classification. Chapman and Hall, London, 193 pp.

Grebmeier, J.M., B.A. Bluhm, L.W. Cooper, S.G. Denisenko, K. Iken, M. Kędra, and C. Serratos, 2015a. Time-series benthic community composition and biomass and associated environmental characteristics in the Chukchi Sea during the RUSALCA 2004–2012 Program. Oceanography 28(3):116–133, doi:10.5670/oceanog.2015.61.

Grebmeier, J.M., B.A. Bluhm, L.W. Cooper, S. Danielson, K.R. Arrigo, A.M. Blanchard, J.T. Clarke, R.H. Day, K.E. Frey, R.R. Gradinger, M. Kedra, B. Konar, K.J. Kuletz, S.H. Lee, J.R. Lovvorn, B.L. Norcross, S.R. Okkonen, 2015b. Ecosystem characteristics and processes facilitating persistent macrobenthic biomass hotspots and associated benthivory in the Pacific Arctic. Prog. Oceanogr., 136, 92-114.

Hill, V., Ardyna, M., Lee, S.H., Varela, D.E., this issue. Decadal trends in phytoplankton production in the Pacific Arctic Region from 1950 to 2012.

Hopcroft, R.R., Day, R.H., 2013. Introduction to the special issue on the ecology of the northeastern Chukchi Sea. Cont. Shelf Res. 67, 1–4.

Hunt, G.L., Blanchard, A.L., Boveng, P., Dalpadado, P., Drinkwater, K.F., Eisner, L., Hopcroft, R.R., Kovacs, K.M., Norcross, B.L., Renaud, P., Reigstad, M., 2013. The Barents and Chukchi Seas: Comparison of two Arctic shelf ecosystems. J. Mar. Syst. 109, 43–68.

Itoh, M., Pickart, R.S., Kikuchi, T., Fukamachi, Y., Ohshima, K.I., Simizu, D., Arrigo, K.R., Vagle, S., He, J., Ashjian, C., JMathis, J.T., Nishino, S., and Nobre, C. 2015. Water properties, heat and volume fluxes of Pacific water in Barrow Canyon during summer 2010. *Deep-Sea Research I* 102, 43-54.

Kuletz, K.J., M.C. Ferguson, B. Hurley, A.E. Gall, E.A. Labunski, T.C. Morgan. 2015. Seasonal spatial patterns in seabird and marine mammal distribution in the eastern Chukchi and western Beaufort seas: identifying biologically important pelagic areas. Prog. Oceanogr., 136 (2015), 175-200, 10.1016/j.pocean.2015.05.012

Ladd, C., Mordy, C.W., Salo, S.A., Stabeno, P.J., 2016. Winter water properties and the Chukchi polynya. J. Geophys. Res. 121, 5516–5534, doi:10.1002/2016JC011918.

Laurel, B.J., Spencer, M., Iseri, P., Copeman, L.A. 2016. Temperature-dependent growth and behavior of juvenile Arctic cod (Boreogadus saida) and co-occuring north Pacific gadids. Polar Biology 39:1127-1135.

Logerwell, E., Busby, M., Carothers, C., Cotton, S., Duffy-Anderson, J., Farley, E., Goddard, P., Heintz, R., Holladay, B., Horne, J., Johnson, S., Lauth., B. Moulton, L., Neff., D., Norcross, B., Parker-Stetter, S., Seigle, J., Sformo, T. 2015. Fish communities across a spectrum of habitats in the western Beaufort Sea and Chukchi Sea. Prog. Oceanogr. 136,115-132.

Moore, S.E., Stabeno, P.J., 2015. Synthesis of Arctic Research (SOAR) in marine ecosystems of the Pacific Arctic. Prog. Oceanogr. 136, 1-11, doi:10.1016/j.pocean.2015.05.017.

Moore, S.E., Stabeno, P.J., Grebmeier, J.M., Okkonen, S.R., this issue. The Arctic Marine Pulses Model: Linking annual oceanographic processes to contiguous ecological domains in the Pacific Arctic. Deep-Sea Res. Part II..

Norcross, B.L., Holladay, B.A., Busby, M.S., Mier, K.L., 2010. Demersal and larval fish assemblages in the Chukchi Sea. Deep-Sea Res. II 57: 57-70.

Overland, J.E., Wang, M., 2010. Large-scale atmospheric circulation changes are associated with the recent loss of Arctic sea ice. Tellus A 62, 1–9, doi:10.1111/j.1600-0870.2009.00421.x.

Paquette, R.G., Bourke, R.H., 1974. Observations on the coastal current of arctic Alaska. J. Mar. Res. 32, 195–207.

Pisareva, M.N., Pickart, R.S., Iken, K., Ershova, E.A., Grebmeier, J.M., Cooper, L.W., Bluhm, B.A., Nobre, C., Hopcroft, R.R., Hu, H., Wang, J., Ashjian, C.J., Kosobokova, K.N., Whitledge, T.E., 2015. The relationship between patterns of benthic fauna and zooplankton in the Chukchi Sea and physical forcing. Oceanography 28(3), 69–82.

Pinchuk, A.I., and Eisner, L.B. 2017. Spatial heterogeneity in zooplankton summer distribution in the eastern Chukchi Sea in 2012-2013 as a result of large-scale interactions of water masses. Deep-Sea Res. II 135:27-39.

Questel, J.M., Clarke, C., Hopcroft, R.R., 2013. Seasonal and interannual variation in the planktonic communities of the northeastern Chukchi Sea during the summer and early fall. Cont. Shelf Res. 67, 23–41.

Robertson, A.W., Ghil, M., 1999. Large-scale weather regimes and local climate over the western United States. J. Climate 12, 1796–1813.

Shimada, K., Kamoshida, T., Itoh, M., Nishino, S., Carmack, E., McLauglin, F., Zimmerman, S., and Proshutinsky, A., 2006. Pacific Ocean inflow: Influence on catastrophic reduction of sea ice cover in the Arctic Ocean. Geophys. Res. Lett., 33,L08605, doi:10.1029/2005/GL025624.

Sigler, M., Mueter, F., Bluhn, B., Busby, M., Cokelet, E., Danielson, S., DeRobertis, A., Eisner, L., Farley, E., Iken, K., Kuletz, K., Lauth, R., Logerwell, E., Pinchuk, A., 2017. Late summer zoogeography of the northern Bering and Chukchi seas. Deep-Sea Res. II, 135:168-189.

Springer, A.M., McRoy, C.P., Turco, K.R., 1989. The paradox of pelagic food webs in the northern Bering Sea, II. Zooplankton communities. Cont. Shelf Res. 9, 359–386.

Stabeno, P., Kachel, N., Ladd, C., and Woodgate, R., 2018. Flow patterns in the eastern Chukchi Sea: 2010–2015. J. Geophys. Res., doi:10.1002/2017JC013135.

Wang, J., Mizobata, K., Bai, X., Hu, H., Jin, M., Yu, Y., M. Ikeda, M., Johnson, W., Perie, W., and Fujisaki, A., 2014. A modeling study of coastal circulation and landfast ice in the nearshore Beaufort and Chukchi seas using CIOM, J. Geophys. Res. Oceans, 119, doi:10.1002/2013JC009258

Weingartner, T.J., Danielson, S., Sasaki, Y., Pavlov, V., Kulakov, M., 1999. The Siberian Coastal Current: A wind- and buoyancy-forced Arctic coastal current. J. Geophys. Res. 104, 29697–29713.

Weingartner, T., Aagaard, K., Woodgate, R., Danielson, S., Sasaki, Y., Cavalieri, D., 2005. Circulation on the north central Chukchi Sea shelf. Deep-Sea Res. II: Top. Stud. Oceanogr. 52, 3150–3174.

Weingartner, T., Dobbins, E., Danielson, S., Winsor, P., Potter, R., Statscewich, H., 2013. Hydrographic variability over the northeastern Chukchi Sea shelf in summer-fall 2008–2010. Cont. Shelf Res. 67, 5–22.

Whitehouse, G.A., Aydin, K., Essington, T.E., Hunt, Jr., G.L. 2014. A trophic mass balance model of the eastern Chukchi Sea with comparisons to other high-latitude systems. Polar Biology 37:911-939.

Winsor, P., and Chapman, D.C., 2004. Pathways of Pacific water across the Chukchi Sea: A numerical model study, J. Geophys. Res., 109, C03002, doi:10.1029/2003JC001962.

Wood, K.R., N.A. Bond, J.E. Overland, S.A. Salo, P. Stabeno, and J. Whitefield, 2015. A decade of environmental change in the Pacific Arctic region. Prog. Oceanogr., 136, 12–31, doi: 10.1016/j.pocean.2015.05.005.

Woodgate, R.A., Aagaard, K., Weingartner, T.J., 2005. Monthly temperature, salinity, and transport variability of the Bering Strait through flow. Geophys. Res. Lett. 32, L04601, doi:10.1029/2004GL021880.

Woodgate, R.A., Weingartner, T.J., Lindsay, R., 2012: Observed increases in Bering Strait oceanic fluxes from the Pacific to the Arctic from 2001 to 2011 and their impacts on the Arctic Ocean water column. Geophys. Res. Lett. 39, doi:10.1029/2012GL054092.

Woodgate, R.A., K.M. Stafford, K.M., and Prahl, F.G., 2015: A synthesis of year-round interdisciplinary mooring measurements in the Bering Strait (1990–2014) and the RUSALCA years (2004–2011). Oceanography 28(3):46–67, doi.org/10.5670/ oceanog.2015.57.

Table 1. Cluster member occurrence by period showing the number (percent) of months associated with each cluster. The bottom two lines are the number months (percent) associated with first half of the record (1979-1996) and the second half of the record (1997-2014).

Cluster	**1**	**2**	**3**	**4**	**5**
June	12 (33%)	7 (19%)	5 (14%)	4 (11%)	8 (22%)
July	9 (25%)	10 (28%)	3 (8%)	8 (22%)	6 (17%)
August	11 (31%)	9 (25%)	3 (8%)	6 (17%)	7 (19%)
September	5 (14%)	11 (31%)	4 (11%)	9 (25%)	7 (19%)
October	8 (22%)	7 (19%)	7 (19%)	6 (17%)	8 (22%)
1979-1996	28 (31%)	23 (26%)	11 (12%)	12 (13%)	16 (18%)
1997-2014	17 (19%)	21 (23%)	11 (12%)	21 (23%)	20 (22%)

Figures

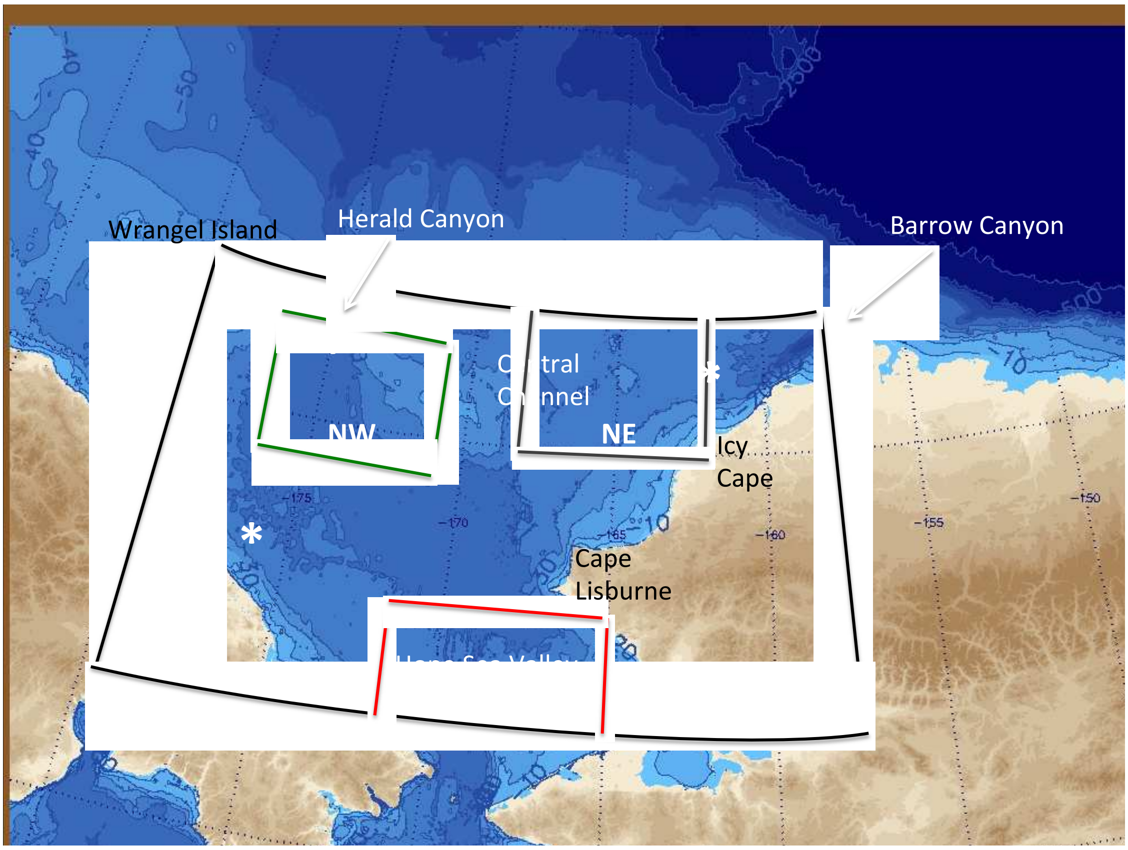

Fig. 1. Chukchi Sea base map (depth contours at 10-m intervals) and region used for cluster analysis (enclosed by solid black lines). The sub-regions used to evaluate temporal variability in heat content are enclosed by red, gray and green boxes and labeled with sub-region name (S, NE, NW). Asterisks (*) show the locations where vertically-integrated currents are evaluated.

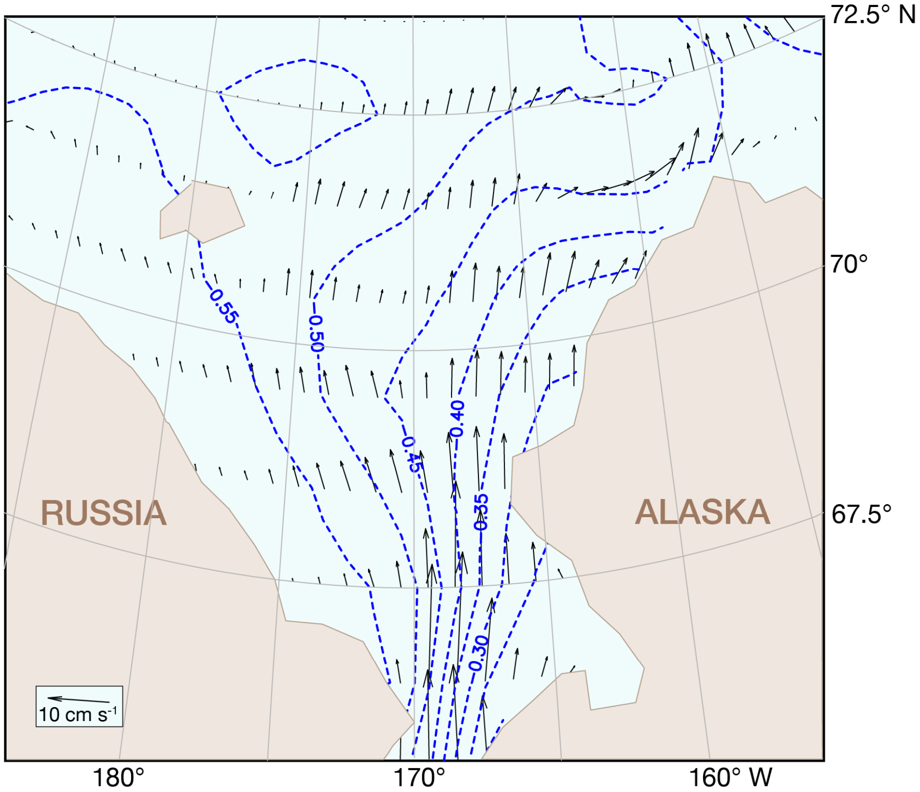

Fig. 2. Mean sea surface height (m, negative values indicated with dashed contours) during June through October 1979–2014. Arrows indicate the mean vertically integrated currents (scale at lower left).

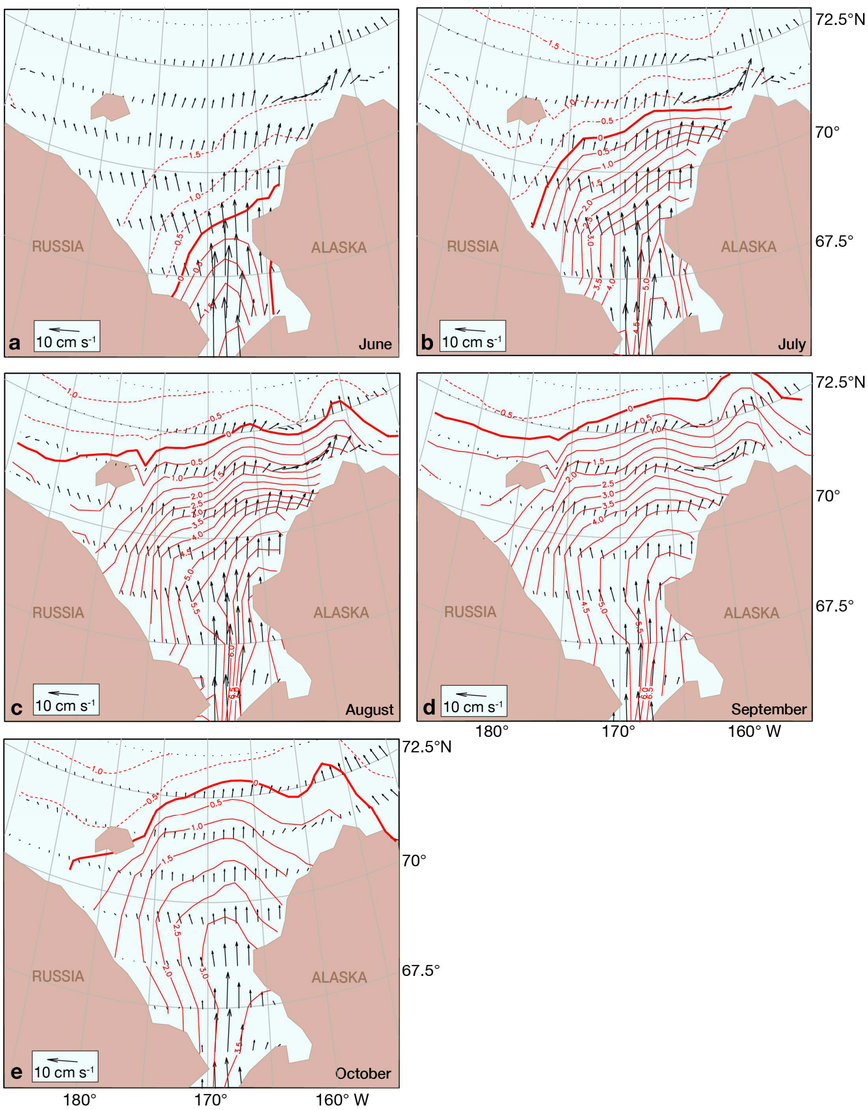

Fig. 3. Mean vertically integrated temperature (contour interval 0.5 °C, negative values indicated by dashed contours) and current vectors (scale at lower left) for the years of 1979 through 2014 during the months of (a) June, (b) July, (c) August, (d) September, and (e) October.

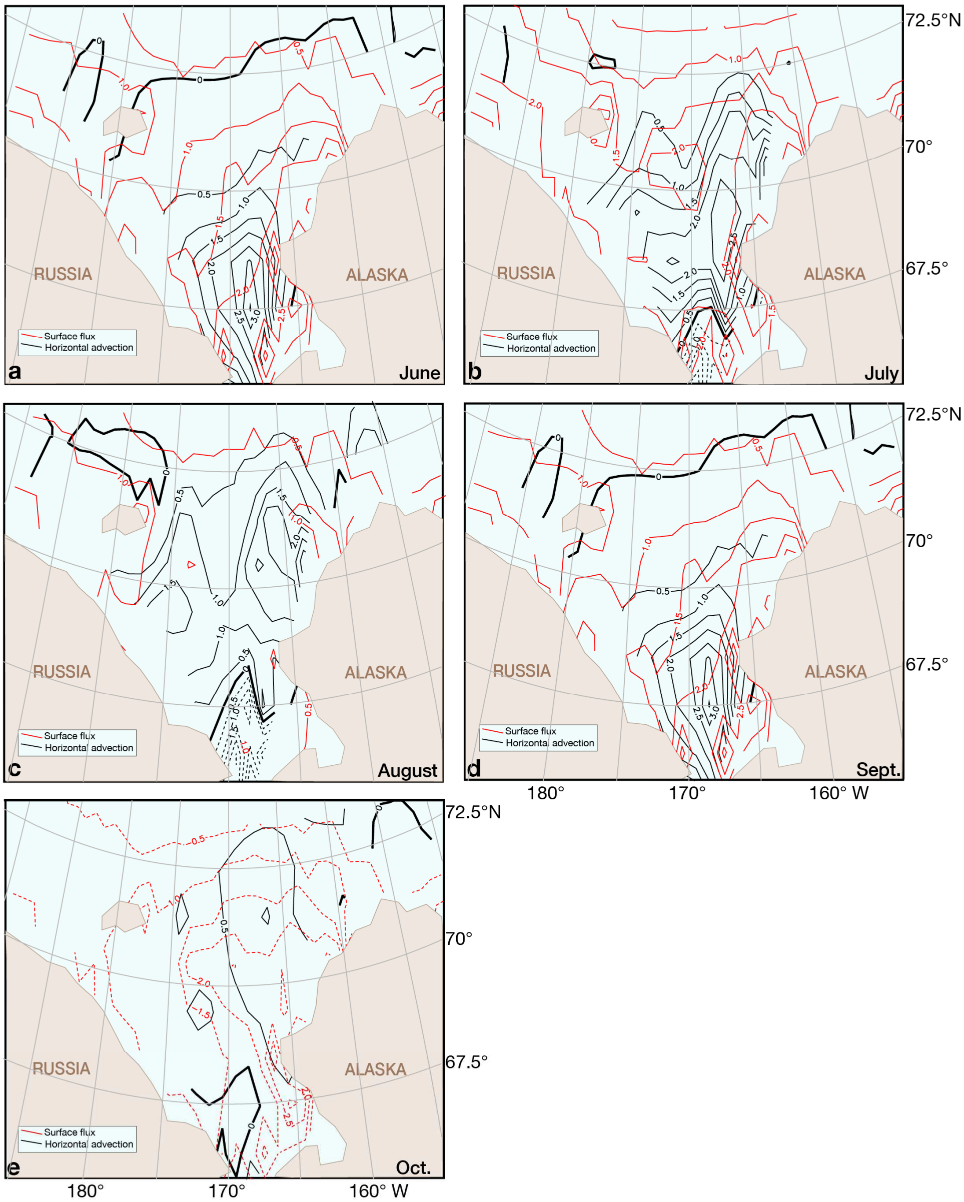

Fig. 4. Mean heating rate (contour interval 0.5 °C per month; negative values indicated by dashed contours) due to the net surface heat fluxes (red) and horizontal advection (black) for the years of 1979 through 2014 during the months of: (a) June, (b) July, (c) August, (d) September, and (e) October.

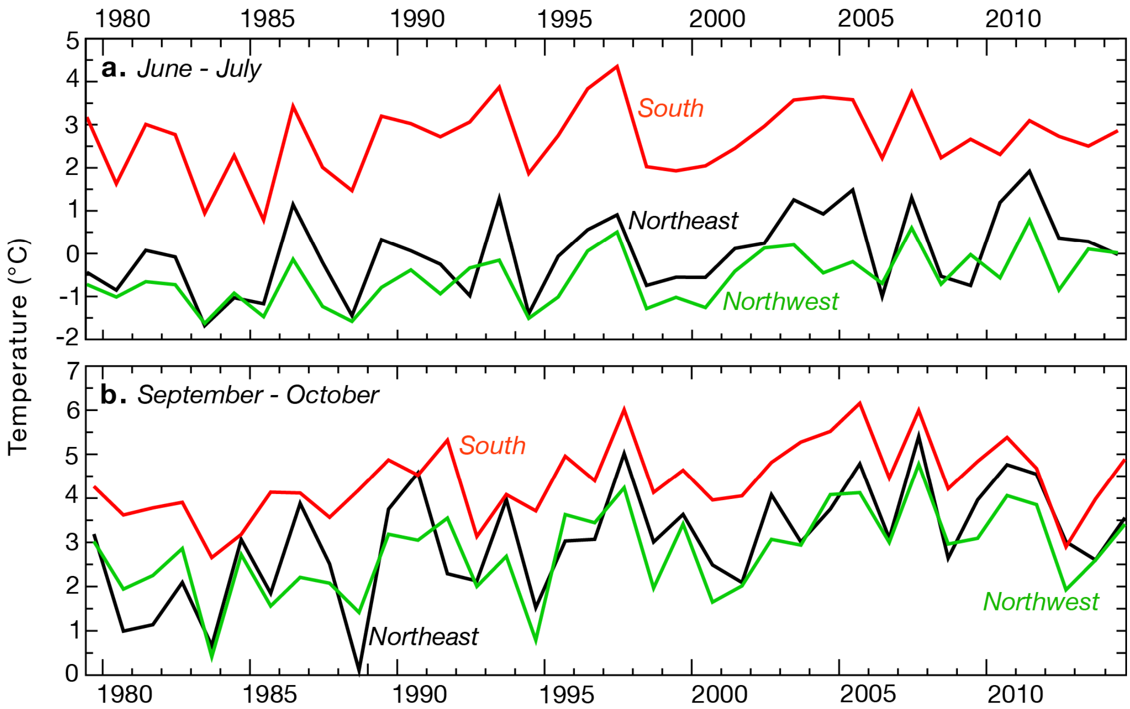

Fig. 5. Time series of vertically averaged temperatures during (a) June–July and (b) September–October from 1979 to 2014 for regions in the southern (red), northeastern (black), and northwestern (green) areas of the Chukchi Sea (shown in Fig. 1). These regions are indicated in Fig. 1 by the boxes labeled S, NE, and NW, respectively.

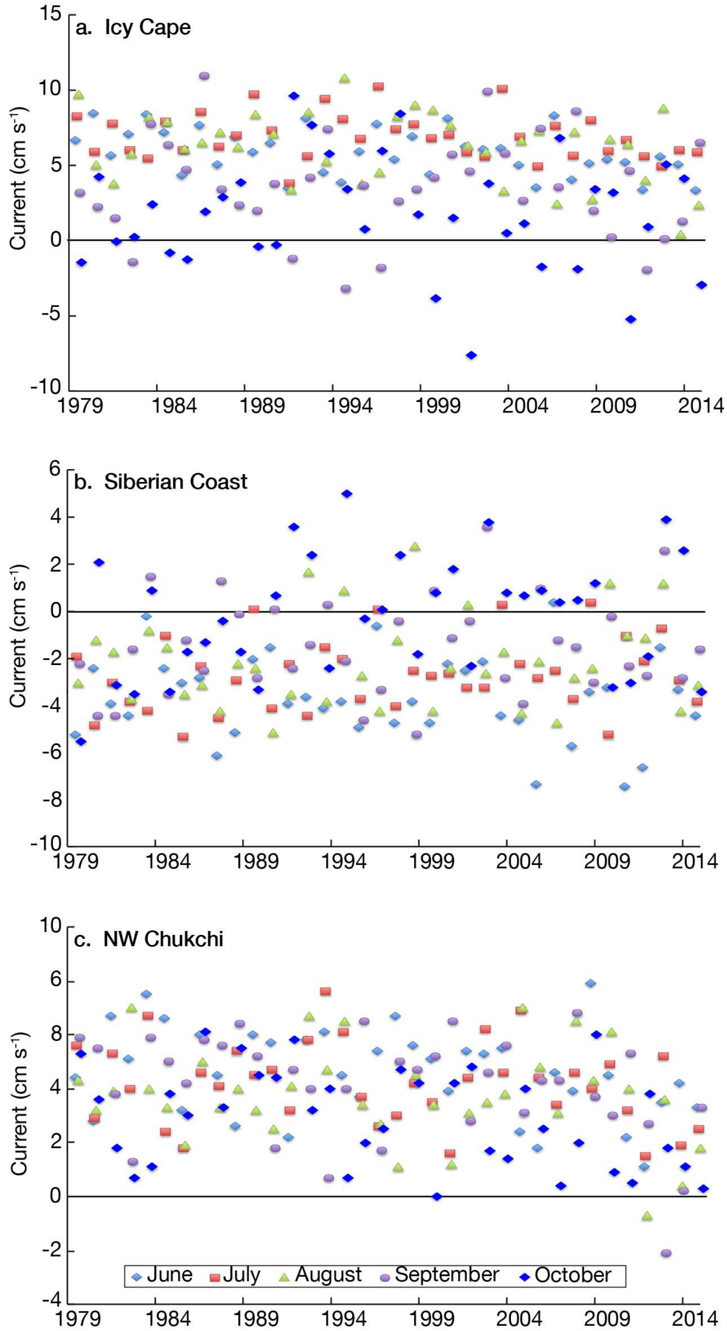

Fig. 6. Monthly values of vertically integrated along-coast current at: (a) 71°N, 162°W near Icy Cape, where positive (negative) values indicate flow toward the northeast (southwest); (b) at 68.5°N, 176°W near the Siberian coast where positive (negative) values indicate flow toward the east-southeast (west-northwest); and (c) meridional flow at 71°N, 175°W in the NW Chukchi Sea. Locations of measurements are indicated with a * in Fig. 1. Symbols for the months of June through October are shown in the legend at the bottom of (c). Note the different vertical scales.

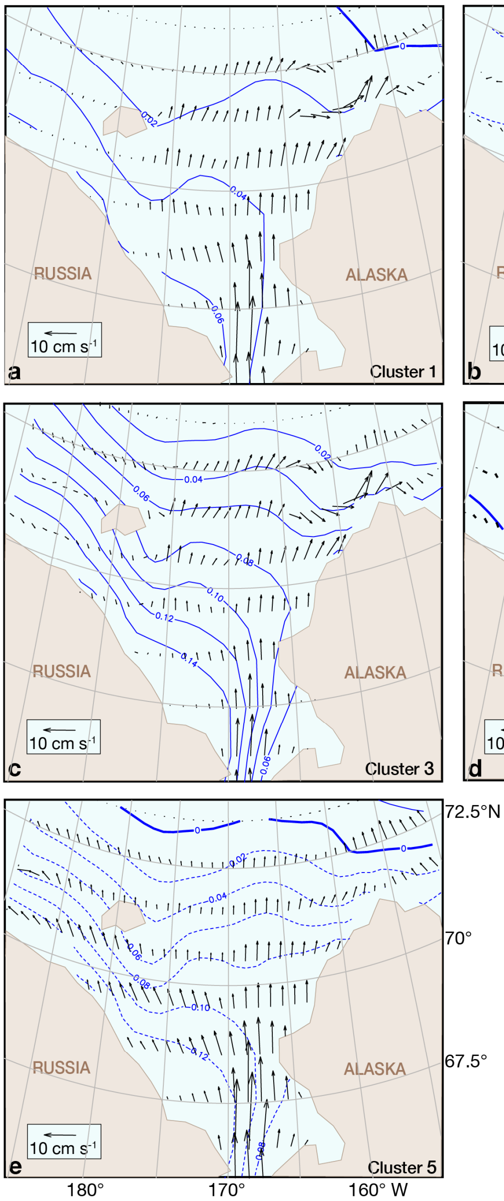

Fig. 7. Composite SSH anomaly (contour interval 0.02 m, negative values indicated by dashed contours) and mean vertically integrated current vectors (scale at lower left) during months designated in (a) Cluster 1, (b) Cluster 2, (c) Cluster 3, (d) Cluster 4, and (e) Cluster 5.

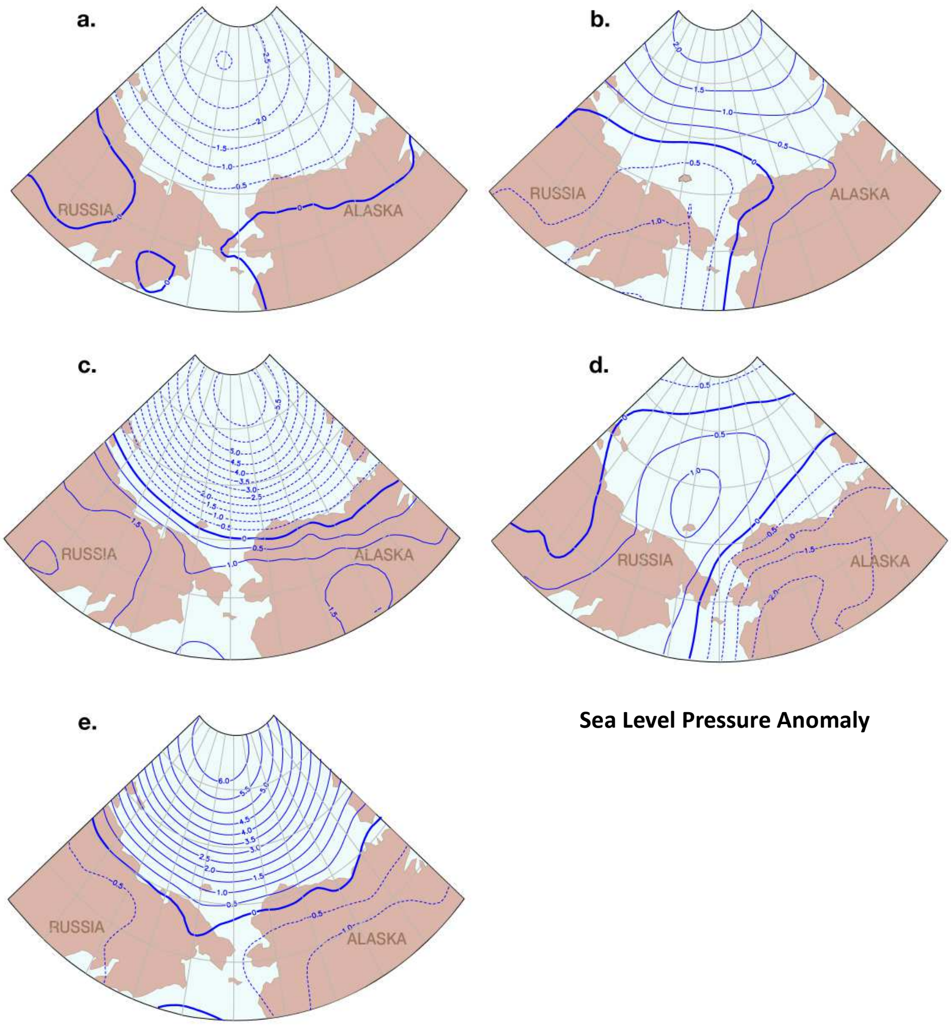

Fig. 8. Composite sea level pressure anomaly (contour interval: 0.5 hPa, negative values indicated by dashed contours) during months designated in (a) Cluster 1, (b) Cluster 2, (c) Cluster 3, (d) Cluster 4, and (e) Cluster 5.

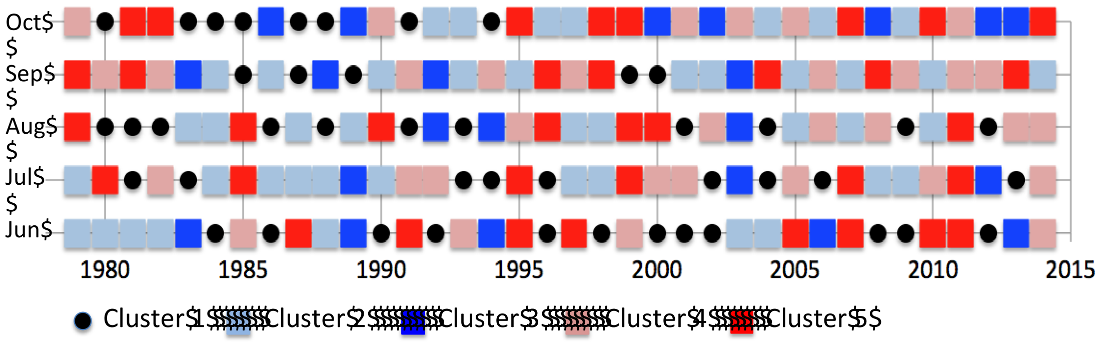

Fig. 9. Temporal distribution by year (horizontal axis) and month (vertical axis) of cluster members 1 (black dots), 2 (light blue squares), 3 (blue squares), 4 (pink squares), and 5 (red squares).

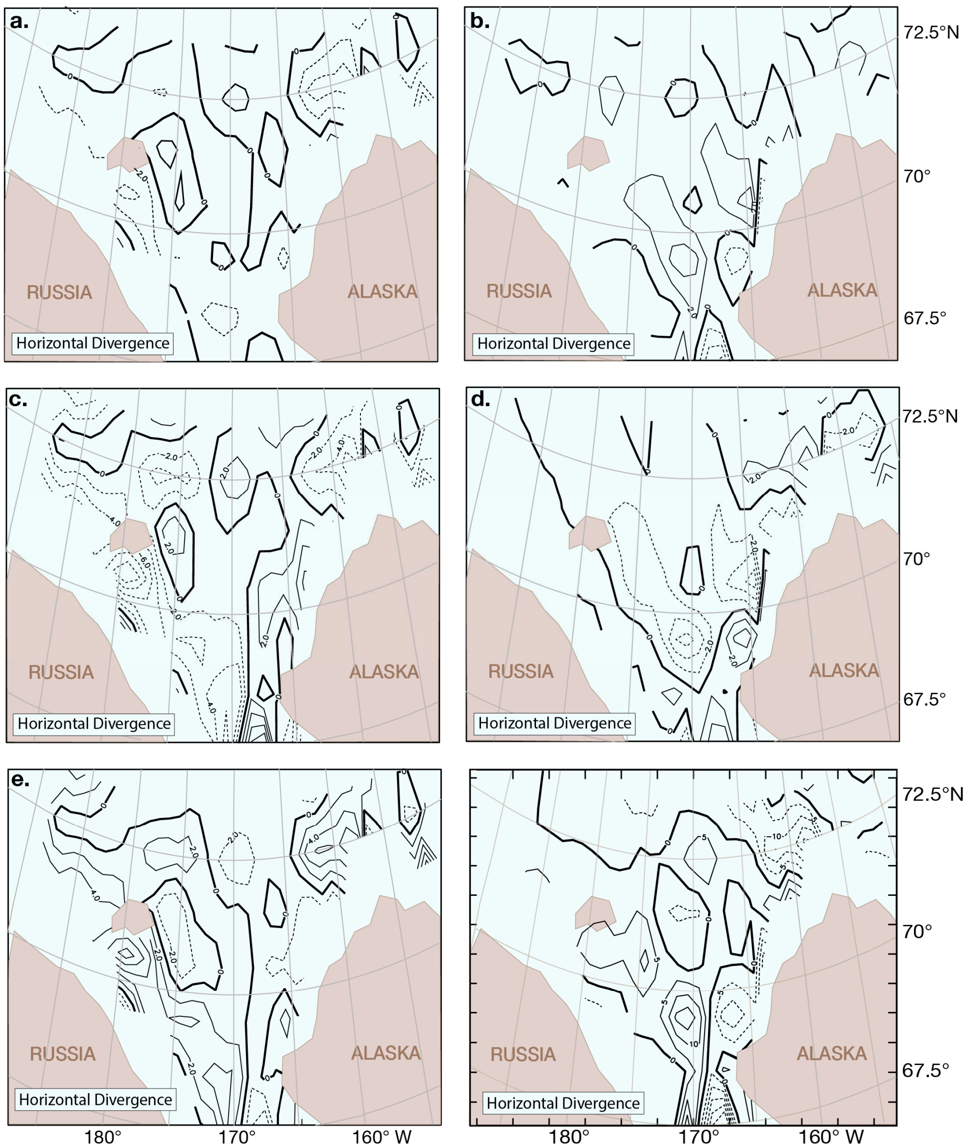

Fig. 10. Composite horizontal divergence anomaly in the upper 20 m of the water column (contour interval 2×10^{-8} s^{-1}, negative values indicated by dashed contours) during months designated in (a) Cluster 1, (b) Cluster 2, (c) Cluster 3, (d) Cluster 4, and (e) Cluster 5. The mean horizontal divergence in the upper 20 m of the water column (contour interval 5×10^{-8} s^{-1}, negative values indicated by dashed contours) is shown for comparison in the lower-right panel.